Annual Progress Report for

Grant NAG 5-2346

Titled

GEOTAIL MCA PLASMA WAVE INVESTIGATION DATA ANALYSIS

Covering the reporting period

August 15, 1996 to August 14, 1997

Submitted to

National Aeronautics and Space Administration
Goddard Space Flight Center

by

Roger R. Anderson
Principal Investigator

June 1997

Department of Physics and Astronomy
The University of Iowa
Iowa City, IA 52242-1479
Telephone: 319/335-1924
FAX: 319/335-1753

INTRODUCTION

This report is for NASA Grant NAG 5-2346, GEOTAIL MCA Plasma Wave Investigation Data Analysis. This report covers the time period August 15, 1996, to August 14, 1997. NASA Grant NAG 5-2346 from Goddard Space Flight Center (GSFC) supports the data reduction and analysis effort at The University of Iowa for the ISTP/GGS GEOTAIL Multi-Channel Analyzer (MCA) which is a part of the GEOTAIL Plasma Wave Instrument (PWI). The primary goals of the International Solar Terrestrial Physics/Global Geospace Science (ISTP/GGS) program are identifying, studying, and understanding the source, movement, and dissipation of plasma mass, momentum, and energy between the Sun and the Earth. The GEOTAIL spacecraft was built by the Japanese Institute of Space and Astronautical Science and has provided extensive measurements of entry, storage, acceleration, and transport in the geomagnetic tail and throughout the Earth's outer magnetosphere. GEOTAIL was launched on July 24, 1992, and began its scientific mission with eighteen extensions into the deep-tail region with apogees ranging from around 60 R_e to more than 208 R_e in the period up to late 1994. Due to the nature of the GEOTAIL trajectory which kept the spacecraft passing into the deep tail, GEOTAIL also made "magnetopause skimming passes" which allowed measurements in the outer magnetosphere, magnetopause, magnetosheath, bow shock, and upstream solar wind regions as well as in the lobe, magnetosheath, boundary layers, and central plasma sheet regions of the tail. In late 1994, after spending nearly 30 months primarily traversing the deep tail region, GEOTAIL began its near-Earth phase. Perigee was reduced to 10 R_e and apogee first to 50 R_e and finally to 30 R_e in early 1995. This orbit provides many more opportunities for GEOTAIL to explore the upstream solar wind, bow shock, magnetosheath, magnetopause, and outer magnetosphere as well as the near-Earth tail regions. The WIND spacecraft was launched on November 1, 1994 and the POLAR spacecraft was launched on February 24, 1996. These successful launches have dramatically increased the opportunities for GEOTAIL and the GGS spacecraft to be used to conduct the global research for which the ISTP program was designed.

The measurement and study of plasma waves have made and will continue to make important contributions to reaching the ISTP/GGS goals and solving the significant problems of sun-earth connections. Plasma waves are involved in the energization and de-energization of plasma and energetic particles via numerous wave-particle interaction processes. Plasma waves in many instances are the source for the heating or cooling of the particles. They can cause particle precipitation by scattering particles into the loss cone. They move particles across boundaries in mass and energy dependent ways. Identifying the waves and the instabilities which produce them are thus crucial for understanding the plasma processes. Wave-particle interaction processes are especially important at various boundaries between the different regions of geospace including the bow shock, magnetopause, and interfaces in the geomagnetic tail between the magnetosheath, lobe, plasmasheet, boundary layers, and neutral sheet. In addition to identifying the characteristics of the instabilities and generation mechanisms encountered, plasma wave measurements are used in conjunction with other fields and particle measurements to identify the region of space the spacecraft is in or the

boundary that is being crossed. For example, the detection of intense low frequency electromagnetic waves is usually indicative of the presence of strong currents found at many boundaries. Observations of the low frequency MCA magnetic field data have been used in the regime identification study reported in Eastman et al. [1997]. Plasma wave emissions can also be used to quantify the plasma density as well. Plasma wave measurements of upper hybrid resonance frequency emissions in the magnetosphere, plasma frequency emissions in the solar wind and magnetosheath, and plasma frequency cutoffs in the tail lobe, plasma sheet, and boundary layer regions provide accurate measurements of plasma density independent of spacecraft charging. In fact, particle experiments use the PWI derived density to calibrate their instruments. Observations of Auroral Kilometric Radiation (AKR) provide a remote indicator of the timing and strengths of geomagnetic storms and substorms. Observations of electromagnetic escaping continuum radiation can provide remote tracking of the movement of injected plasmas during geomagnetic storms and substorms.

MCA PWI EXPERIMENT and INVESTIGATION DESCRIPTION and STATUS

An important part of the experiment complement on GEOTAIL is the Plasma Wave Instrument for which Professor Hiroshi Matsumoto of Kyoto University is Principal Investigator. The three major components of the GEOTAIL PWI are the Multi-Channel Analyzer the Sweep Frequency Analyzer (SFA) and the Waveform Capture (WFC) system. The United States National Aeronautics and Space Administration (NASA) provided the MCA portion of PWI under contract to The University of Iowa for which Dr. Roger R. Anderson is Principal Investigator and U. S. Lead Investigator for the U. S. GEOTAIL MCA Investigation. Dr. Anderson is a Co-Investigator on the GEOTAIL PWI. Dr. Anderson has two Co-Investigators on the U. S. GEOTAIL MCA Investigation: Professor Donald A. Gurnett of The University of Iowa and Dr. William W. L. Taylor of Hughes STX Corporation.

The MCA includes a 20-channel Electric Spectrum Analyzer covering the frequency range from 5.6 Hz to 311 kHz with broadband filters spaced logarithmically (four filters per decade in frequency) and a 14-channel Magnetic Spectrum Analyzer covering the frequency range from 5.6 Hz to 10 kHz with identical filters. The SFA has five electric bands (Band 1: 25 Hz to 200 Hz, Band 2: 200 Hz to 1.6 kHz, Band 3: 1.6 kHz to 12.5 kHz, Band 4: 12.5 kHz to 100 kHz and Band 5: 100 kHz to 800 kHz). The SFA has three magnetic bands identical to the electric bands 1, 2, and 3. Each band has 128 steps spaced linearly in frequency. The sweep rate is 128 steps in 64 seconds for bands 1 and 2 and 8 seconds for bands 3, 4, and 5. The WFC system measures the waveform from the three magnetic search coil sensors and the two electric antennae at a rate of 12000 samples per second for each component. The WFC provides spectra from 10 Hz to 4 kHz. A detailed description of the entire PWI experiment and the initial results are contained in Matsumoto et al. [1994]. It is important to note that the three PWI systems are quite complementary to each other. The MCA provides continuous high-time resolution with broad frequency resolution while the PWI SFA provides high-frequency resolution but coarse time resolution. Another advantage of the MCA is that it measures down to 5 Hz while the SFA begins at 24 Hz. The low

frequency range of the MCA has provided an abundant amount of interesting electromagnetic data in the 5 Hz to 20 Hz range not reachable by the SFA. Data from both the MCA and SFA are used to identify periods from which the PWI WFC data analysis efforts should be concentrated. The WFC provides both high-time resolution and high-frequency resolution but only for very limited periods.

All parts of the GEOTAIL Plasma Wave Instrument including the MCA, the SFA and the WFC system have operated perfectly since the GEOTAIL launch on July 24, 1992. The WANT (Wire ANTenna) and PANT (Probe ANTenna) electric antennas were each successfully deployed on August 27, 1992, to their 100 meter tip-to-tip lengths. The MAST antennas for the Flux-gate and Search Coil magnetometers were deployed to their full lengths on September 16, 1992. Nearly continuous low-bit-rate Editor-B tape-recorded data (complete 20-channel Electric and 14-Channel Magnetic spectra every 1/2 second from the MCA and 5-Band Electric and 3-Band Magnetic spectra every 8 to 64 seconds from the SFA) have been acquired from the GEOTAIL PWI since early September 1992. Approximately eight hours per day of high-bit-rate Editor-A Real Time data (complete Electric and Magnetic spectra every 1/4 second from the MCA, 5-Band Electric and 3-Band Magnetic spectra every 8 to 64 seconds from the SFA, and 8.7 seconds of 5-Component WFC data every 275 seconds) have also been accumulated since early September, 1992. Many new interesting phenomena have been detected during these orbits using the PWI MCA, SFA, and WFC measurements.

Much has been accomplished under Grant NAG 5-2346 for GEOTAIL MCA PLASMA WAVE INVESTIGATION DATA ANALYSIS over the past year. We have maintained and improved the programs for plotting all the real-time MCA and SFA data we collect in appropriate length color spectrogram plots for each daily pass and all of the SIRIUS data in 24-hour plots. The plots are surveyed to find time periods of interest to concentrate on for more detailed studies and collaborations. We have used the Key Parameter Visualization Tool software provided by the CDHF and the Science Planning and Operations Facility (SPOF) at GSFC to plot Key Parameter data from the CANOPUS instrumentation in order to identify substorm onsets and other time periods of interest. We use the World Wide Web (WWW) to examine the WIND/WAVES summary plots in order to compare them with the GEOTAIL observations. The POLAR PWI survey plots are also examined to find time periods of interest. We also use the WWW to look at POLAR VIS images and other GGS/ISTP data sets during time periods of interest. Our programmers have also developed programs and provided technical support for the GEOTAIL data analysis efforts of Co-Investigator William W. L. Taylor.

OBSERVATIONS and RESULTS

Many exciting things have already been observed from our studying these various data sources and we are continuing detailed collaborations with the other GEOTAIL experiments, other members of the GEOTAIL Plasma Wave Team, as well as experimenters from other spacecraft presently operating including POLAR, WIND, IMP-J, GOES, and Galileo, and

from ground observing sites such as the CANOPUS network. Details of the progress we have made and many of the interesting and significant results we have obtained from our research over the past year will be discussed below.

AURORAL KILOMETRIC RADIATION

Much of our interest has been on AKR because it is the plasma wave phenomenon most frequently observed by GEOTAIL and the one most closely related to substorms. A 38-month data set of GEOTAIL plasma wave observations of AKR at 200 kHz and 500 kHz was used in Kasaba et al. [1997b] to examine the dependence of the angular distribution of AKR. Several important results confirmed and expanded on results from previous studies. One was the finding that the illumination region for the low frequency AKR range extends larger than that for the high frequency range. Such difference is basically explained by propagation. Another was finding that the equatorward extension of the illumination region for large Kp is caused by the equatorward shift of the auroral plasma cavity in the disturbed phase which should be related to the inward motion of the plasmapause just after the onset of substorms.

Several important new results were also found. One was the fact that the illumination region of AKR extends duskward as geomagnetic conditions become more disturbed especially for the low frequency range. This suggests the duskward extension of the AKR source. Lack of such feature at the high frequency range could be caused by insufficient density depression in the duskside auroral plasma cavity especially at lower altitudes. The primary generation mechanism presently considered for AKR, the electron cyclotron maser instability, requires a small plasma frequency to cyclotron frequency ratio. AKR is believed to be generated near the local electron cyclotron frequency such that high frequency AKR is generated at a lower altitude than the low frequency AKR. In the duskside plasmasphere, the electron density is enhanced so that the density in the auroral plasma cavity should be hard to decrease enough to satisfy the condition for the electron cyclotron maser instability. Therefore, generation of high-frequency AKR at lower altitudes is expected to be blocked on the duskside hemisphere.

A second new result was that the frequency of occurrence of AKR depends on observed time in UT which approximately corresponds to the longitude of the source especially for the high frequency range. The longitudinal dependence is evident in the same manner as shown in the optical auroral activity. This suggests that populations of energetic electrons are controlled by the altitude of the magnetic mirror point especially at lower altitudes. Another new result was that AKR is more active on the winter hemisphere especially for the high frequency range. Possible reasons include asymmetry of the population of precipitating electrons on the auroral field lines and insufficient density depression in the auroral plasma cavity on the summer hemisphere especially at lower altitudes which are most sensitive to ionospheric outflow. This study highlighted the fact that remote satellite observations can suggest the population of energetic electrons and the structure of the auroral plasma cavity on

the auroral field lines which should be sensitive to the plasma density in the surrounding plasmasphere.

LOW FREQUENCY BURSTS and SUBSTORMS

GEOTAIL PWI measurements along with those from the WIND WAVES experiment, the POLAR PWI, and GOES 8 along with CANOPUS and National Geophysical Data Center (NGDC) magnetograms have provided new information on terrestrial low frequency (LF) bursts [Anderson et al. 1997a,b]. We have found that they are intimately related to AKR and are produced simultaneously with intense isolated substorms. The AKR is enhanced both in intensity and frequently in both the lower and upper frequency extent. This implies that the AKR generation region moves to both higher and lower altitudes during the isolated substorms. The absence of higher frequency AKR in some upstream observations of LF bursts can be attributed to propagation blockage by the earth and dense plasmasphere of the portion of the AKR generated at the lowest altitudes on the night side.

We will discuss some of the more interesting observations related to LF bursts that we have made this past year using the GEOTAIL MCA and PWI data. The study of the LF bursts detected between 0500 UT and 0700 UT on April 14, 1996, provides an excellent example of the wealth of information the GGS/ISTP armada of spacecraft and ground stations can focus on solar-terrestrial interactions. This is illustrated in Figure 1 which shows the radio and plasma wave data from three spacecraft and the CANOPUS Key Parameter CL data for that two hour period. The CANOPUS CL data plotted in the bottom panel is the lower trace of the envelope of all magnetograms for the CANOPUS array of ground magnetometers. In an ongoing study we have found that LF bursts were usually associated with substorms featuring strong narrow negative bays, many as deep as -800 to -1000 nT. The negative bay observed in Figure 1 reached a minimum of about -970 nT at 0545 UT.

The first (top) panel of Figure 1 displays the PWI SFA data in two bands with linear frequency scales from 12.5 kHz to 100 kHz and 100 kHz to 800 kHz over a 50 dB dynamic range. The two roughly horizontal lines near 30 kHz and 60 kHz are at the solar wind plasma frequency, F_p, and its second harmonic, $2F_p$. GEOTAIL was in the solar wind just outside the subsolar bow shock with GSEX=18.6 R_e, GSEY=4.6 R_e, GSEZ=-1.5 R_e, and R=19.2 R_e. AKR and the LF burst are identified. The LF burst is strongest above $2F_p$. A weak dispersed low frequency portion of the LF burst is evident from about 60 kHz near 0540 UT down to 30 kHz near 0545 UT.

The second panel of Figure 1 shows the WIND/WAVES RAD1 receiver data on a linear frequency scale from 20 kHz to 800 kHz. Strong AKR up to 500 kHz is prominent. WIND's coordinates were GSEX=50.5 R_e, GSEY=42.3 R_e, GSEZ=-4.6 R_e, and R=66.1 R_e. Being far to the side of the Earth-Sun line, WIND was in a much more favorable position to intercept direct radiation from the AKR source region even though it was farther away. For GEOTAIL, much of the direct radiation from the AKR source region was blocked by the Earth and the dense plasmasphere. The third panel is a Thermal Noise

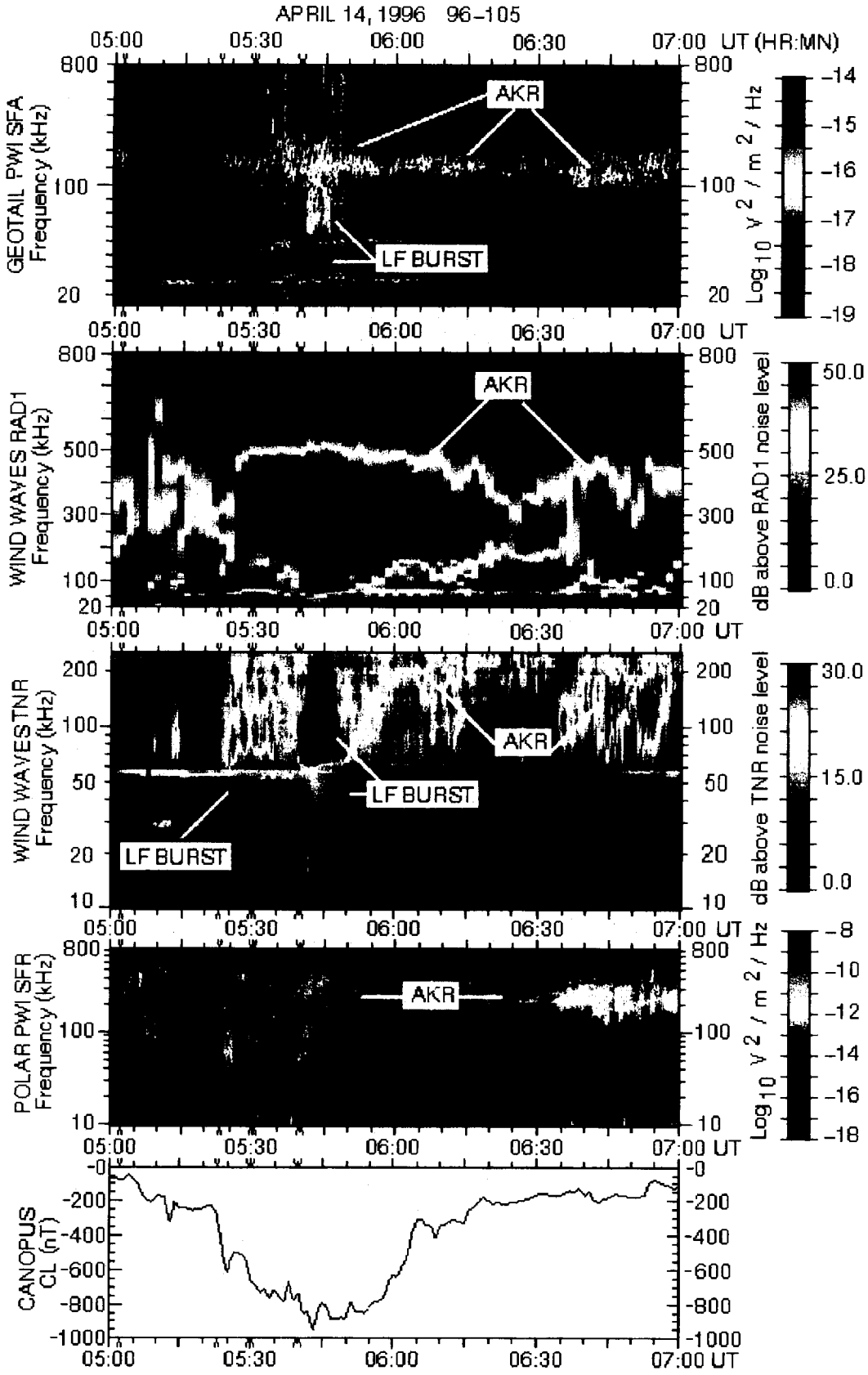
APRIL 14, 1996 96-105
05:00
05:30
06:00
06:30
07:00 UT (HR:MN)
GEOTAIL PWI SFA Frequency (kHz)
AKR
LF BURST
Log10 V2 / m2 / Hz
WIND WAVES RAD1 Frequency (kHz)
dB above RAD1 noise level
WIND WAVES TNR Frequency (kHz)
dB above TNR noise level
POLAR PWI SFR Frequency (kHz)
CANOPUS CL (nT)
07:00 UT

Figure 1

Receiver (TNR) spectrogram from the WIND/WAVES experiment plotted on a logarithmic scale from 4 kHz to 250 kHz and covering a 30 dB dynamic range. The LF burst between 0540 UT and 0545 UT is quite prominent. A weaker LF burst around 0523 UT is also evident.

The fourth panel contains a plot of the electric field data from the POLAR PWI Sweep Frequency Receiver data on a logarithmic frequency scale from 10 kHz to 800 kHz and covers a 100 dB dynamic range. At 0545 UT POLAR was about 6 R_e over the Earth's northern polar region. The AKR burst beginning around 0540 UT clearly extends down to 30 kHz and up to over 500 kHz. When POLAR is high over the polar regions, it provides excellent observations of the total AKR spectrum at its origin which can then be compared to the remote observations of GEOTAIL and WIND. Since AKR is generated near the local electron cyclotron frequency, the higher the AKR frequency, the lower the altitude where it is generated. The Earth and dense plasmasphere block most of the AKR above 300 kHz from reaching GEOTAIL for this event. Note that around 0523 UT when WIND detected a weal LF burst POLAR also detects enhanced AKR down to at least 40 kHz.

The red arrows on the time axis at 0502 UT, 0523 UT, 0530 UT, and 0540 UT indicate when the CANOPUS ground magnetometers showed intensifications indicative of substorm expansive phase onsets. Note that enhanced AKR is detected by POLAR each time. The onsets at 0540 UT were the most intense and most poleward. This could explain the low frequency time dispersion that we see. If the more poleward excursion also corresponds to the disturbance moving to field lines that extend farther out into the magnetosphere, the local AKR frequency will decrease. Frequently we observe that LF bursts are associated with AKR that displays an increasing upper cutoff frequency as well as a decreasing lower cutoff frequency. We believe that a portion of the time dispersion for both the high and low frequency portion of the LF bursts may be due to the movement of the AKR source region. Additional evidence for the substorm timing for this event was found in the GOES 8 magnetometer data. Indications of field aligned currents and magnetic field dipolarizations were found at the same times as the ground magnetometer data onset times. No polar imaging data were available because this event occurred just before a POLAR spin flip when the VIS instrument was safed.

A pair of substorms occurred around 08 UT on January 12, 1997, and were observed by numerous instruments that were a part of the ISTP mission. The GEOTAIL PWI at 28 R_e down the tail and the WIND WAVES experiment upstream at $X=117$ R_e and $Y=-54$ R_e detected enhanced auroral kilometric radiation and a LF burst. GEOTAIL also detected enhanced plasma densities in the plasma sheet and movement of the tail as the spacecraft moved into and out of the lobe. POLAR was inbound at 7.5 R_e near 07 MLT. The POLAR PWI detected the enhanced AKR that included expanded upper and lower frequency cutoffs. Many of the CANOPUS ground magnetometer stations were able to identify both substorms and track their movement. Negative bays near -1000 nT were observed. Large structured injections of protons and electrons were observed by GOES 8 and 9. Images from the POLAR VIS Earth Camera operating in the far-UV range showed a strong aurora with

injections deep into the ring current. These images along with the other observations detail the dynamics of the plasma associated with these strong substorms. Excellent agreement was found between the location of the aurora in the images and the substorm activity detected by the various CANOPUS ground magnetometer sites. The LF burst again occurred as the substorms moved poleward. The excellent agreement between the imaging data and the ground magnetometer data aids us in understanding the substorm dynamics when one or the other data set is not available.

Interesting and sometimes conflicting information about the LF bursts have been found. On April 11, 1997, several LF bursts were identified with substorms following the Coronal Mass Ejection (CME) event beginning a few days earlier. These LF bursts were detected by GEOTAIL, WIND, and POLAR. For the burst occurring between 0300 UT and 0400 UT, GEOTAIL was at XGSE = 13.9 R_e and YGSE = -1.2 just upstream of the Earth's bow shock. GEOTAIL detected the LF burst down to 42 kHz which was just above the solar wind plasma frequency observed to be 40 kHz. On POLAR the LF burst was observed by the Wide Band Receiver in the 0 to 90 kHz mode as well as by the SFR and MCA. On POLAR the LF burst was detected down to 27 kHz. However, while clear spin modulation was evident above about 45 kHz, below 45 kHz the data was isotropic. We need to find additional cases in order to determine whether the lack of spin modulation indicates a different source or just a much broader source region.

A LF burst detected by both GEOTAIL and POLAR on May 15, 1997, shows nearly the same time dispersion for both spacecraft even though POLAR was near the source region and GEOTAIL was near apogee in the dusk magnetosheath. Figure 2 shows a ten-minute interval from 1250 UT to 1300 UT when GEOTAIL was at XGSE = 7.8 R_e and YGSE = 28.6 R_e. The time dispersion at the leading edge of the LF burst is most evident in Band 4 which covers 12.5 kHz to 100 kHz on a linear scale. Figure 3 shows the POLAR data plotted logarithmically from 10 kHz to 800 kHz. Note that the time dispersion appears very similar on both spacecraft even though GEOTAIL was in the magnetosheath. This means that this observed time dispersion is present at the source and is not a propagation and deep tail scattering effect for this case. Also very interesting is the fact that for this case the POLAR data show spin modulation down to at least 30 kHz. The nearly vertical striations in the POLAR spectrogram are due to a beating between the spin period and the data sampling period. The presence of similar spin modulation here for both the high and low frequency components supports the idea the LF burst is a component of AKR. If we assume we are looking at low frequency AKR generated near the electron gyrofrequency, the time dispersion indicates the source region is moving out along the auroral field lines around 30 km/s to 50 km/s.

The GEOTAIL PWI has provided new details on Auroral Myriametric Radiation (AMR) which is a low-frequency radiation which correlates with simultaneously observed AKR emissions. Previous studies had reported on AMR in the 10 - 40 kHz frequency range. The GEOTAIL observations show that the frequencies of such correlated emissions become as low as 1 kHz and may not always be associated with AKR. While almost all of the LF

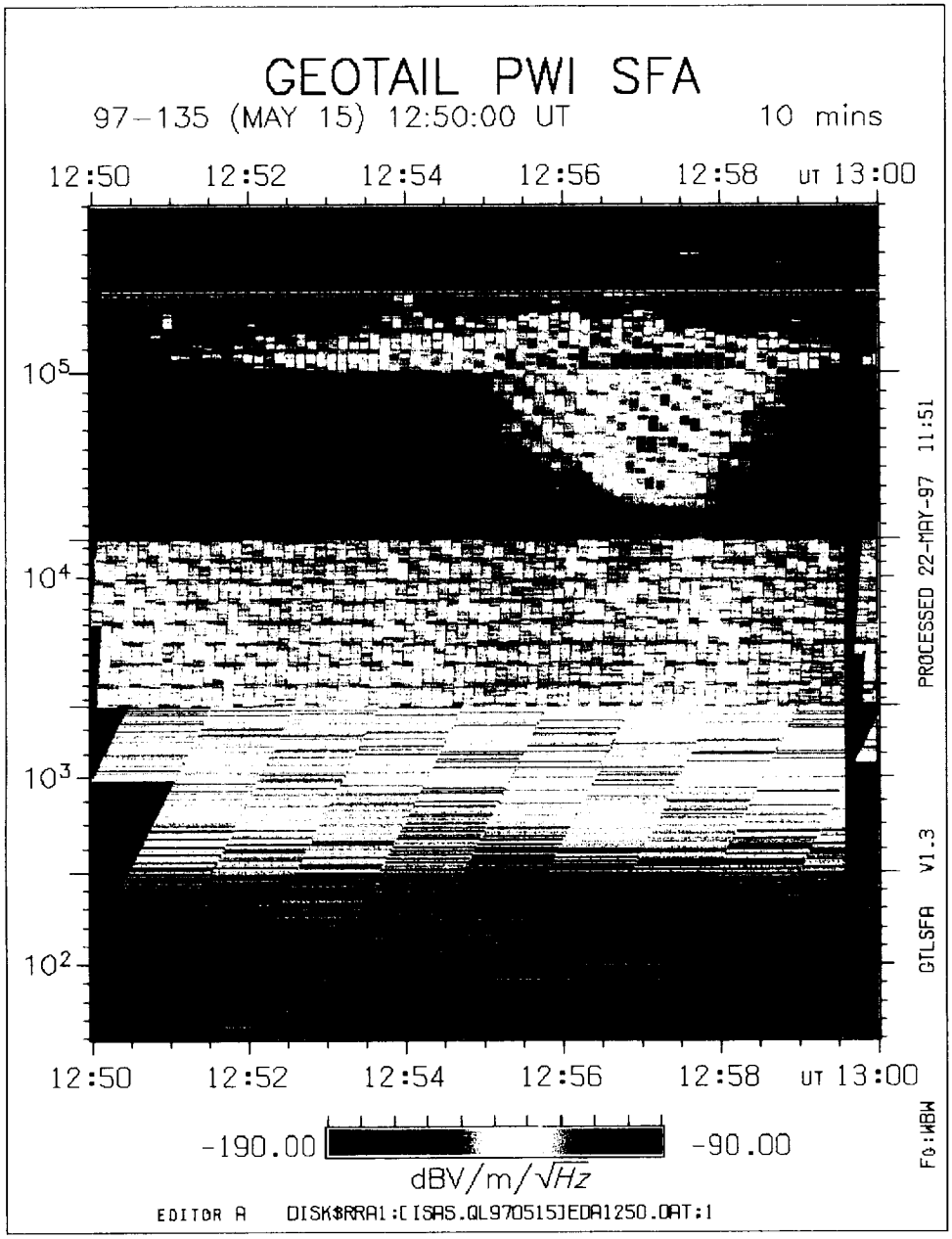
GEOTAIL PWI SFA
97-135 (MAY 15) 12:50:00 UT
10 mins
12:50
12:52
12:54
12:56
12:58
UT 13:00
10^5
10^4
10^3
10^2
PROCESSED 22-MAY-97 11:51
GTLSFA V1.3
FG:WBW
-190.00
-90.00
dBV/m/√Hz
EDITOR A
DISK$RRA1:[ISAS.QL970515]EDA1250.DAT;1

Figure 2

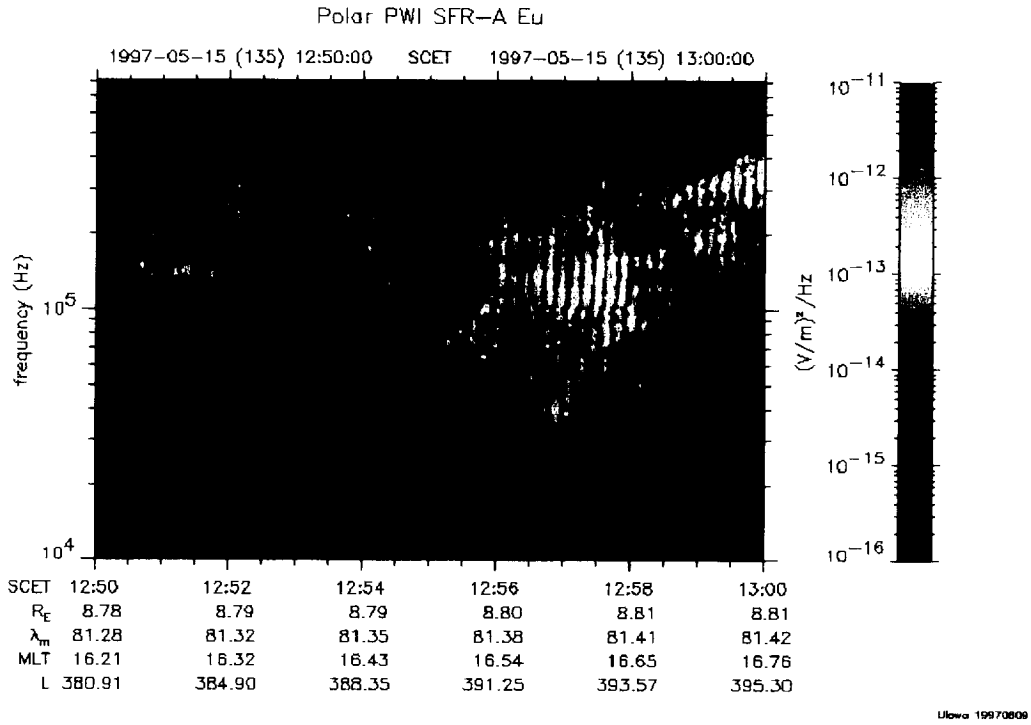
Polar PWI SFR-A Eu
1997-05-15 (135) 12:50:00 SCET 1997-05-15 (135) 13:00:00
frequency (Hz)
10^5
10^4
10^{-11}
10^{-12}
10^{-13}
10^{-14}
10^{-15}
10^{-16}
$(V/m)^2/Hz$
SCET 12:50 12:52 12:54 12:56 12:58 13:00
R_E 8.78 8.79 8.79 8.80 8.81 8.81
λ_m 81.28 81.32 81.35 81.38 81.41 81.42
MLT 16.21 16.32 16.43 16.54 16.65 16.76
L 380.91 384.90 388.35 391.25 393.57 395.30
Uiowa 19970809

Figure 3

bursts we have studied have appeared related to AKR, the observed AKR has not always been continuous from the high frequency portion to the low frequency portion. Sometimes the lower frequency portion of the LF bursts appears more closely related to the AMR.

We will continue the study of the multiple spacecraft and ground observations of the global activity that leads to observations of the LF bursts in order to get meaningful statistics. We will work with Gordon Rostoker on the CANOPUS data, Mike Kaiser and Jean-Louis Bougeret on the WIND/WAVES data, Howard Singer and Terry Onsager on the NOAA GOES and NGDC data, Don Gurnett on the POLAR PWI data, Lou Frank and John Sigwarth on the POLAR VIS data, Jack Scudder on the POLAR HYDRA data, and Hiroshi Matsumoto and Kozo Hashimoto and their colleagues in Japan on the GEOTAIL PWI data. Collaboration with the GEOTAIL CPI, EPIC, MGF, and LEP teams will also be undertaken to better understand the in situ changes observed at GEOTAIL during substorms producing LF bursts. Representatives of POLAR UVI and PIXIE instruments will also be included in studies where their imaging data is used. The goals will be to define the relationship between AKR and LF bursts and to identify the plasma dynamics that produce LF bursts.

ENHANCED CONTINUUM RADIATION

Isolated short-lived bursts of terrestrial myriametric (nonthermal continuum) radiation in a limited frequency range typically from about 10 kHz to 50 kHz and lasting from tens of minutes to a few hours which we call "Continuum Storms" or "Enhanced Continuum" have been observed throughout the tail from as little as a few times per month to several times per day. Enhancements in the continuum radiation were usually closely associated with increased AKR activity indicative of substorms. Some continuum storms occur at constant delay times from the onset of AKR. A detailed study of continuum enhancements observed by GEOTAIL spacecraft from November 1994 to December 1995 has been reported in Kasaba et al. [1997c]. Past studies found that this radiation is generated at the nightside plasmapause by electrons associated with substorms injected into the local midnight zone. We used this radiation as a remote sensing probe for studying the physical processes around the plasmapause during substorms. We found that classical continuum generated at the dayside plasmapause is sometimes observed following the continuum enhancement. This indicates that both are generated by a series of injected electrons associated with the same substorm. Typical interval between the onset of both radiations is about one hour, which is consistent with the time lag expected from gradient and curvature drift motion of injected electrons. We also found that some of the continuum enhancements consist of "fast" and "main" components, which are distinguished by duration time and rising rate in frequency. We surmise that the fast component is generated first at the plasmapause in local midnight zone by lower energy electrons, while the main component is later generated at the dawnside plasmapause by higher energy electrons. We also found that the radial distance of the source on the plasmapause, estimated from the spacing of banded frequency structure of the continuum enhancement, generally decreases at a rate of -0.5 to -1.0 R_e/h for the first one hour after each substorm. Furthermore, we found that the radial distance of the source sometimes increases at a rate of +0.1 to +0.5 R_e/h for the next one hour associated with

isolated substorms in relative quiet phase. The former suggests that long-term decrease of radius of the plasmapause can be separated into fast ones associated with substorms, while the latter suggests that short-term variations of radius of the plasmapause during each substorms is caused not only by the peeling off but also by compression and recovery of the plasmasphere.

We will continue the study of enhanced continuum since it helps identify plasma motions during substorms. The observations of structured and multiple continuum enhancements by GEOTAIL during substorms offer remote tracking of injected plasmas. The continuum is produced at high density gradients found at the plasmapause (and also the magnetopause) as the injected plasmas impinge on them. We have interpreted the observation of enhanced continuum with more than one rising feature with different slopes as being due to multiple paths for the injected electrons. We will compare the features of the continuum storms observed on GEOTAIL with auroral imaging available from POLAR VIS, UVI, and PIXIE as well as magnetospheric imaging of the Energetic Neutral Atoms (ENA) being carried out using the POLAR CEPPAD. We will attempt to verify the inferences from the PWI data on the plasma motions observed by the imagers. We will also study individual station magnetograms from CANOPUS with the assistance of Gordon Rostoker in order to understand the relationships of the substorm dynamics to the characteristics of the various continuum storms. We have already found the somewhat unexpected result that the continuum storms are typically associated with modest negative bays of the order of only about -200 to -300 nT.

WAVE-PARTICLE INTERACTIONS

Verification of the Kennel and Petschek doppler shifted electron cyclotron resonance whistler-mode wave-particle interaction was obtained for chorus emissions detected by the GEOTAIL PWI and correlated with growth rates calculated from electron distribution functions measured by the GEOTAIL Comprehensive Plasma Instrument (CPI) . Three-dimensional electron velocity distribution functions and plasma wave data acquired from GEOTAIL in the Earth's outer magnetosphere were used to correlate linear cyclotron growth rates and the activity of chorus to show that the nonlinear chorus emissions are generated initially by a linear cyclotron interaction [Yagitani et al., 1996]. The GEOTAIL PWI has also observed chorus triggered by ULF emissions near the dayside magnetopause for a period of eight hours. The WFC receiver data were used to determine the characteristics of the chorus emission, such as the wave normal direction, polarization, refractive index and Poynting flux. The wave normal directions of the chorus were not always parallel to the earth's magnetic field. Wave-particle interactions in the magnetosheath and magnetosphere will continue to be studied. In the outer magnetosphere near the magnetopause we have seen extended periods alternating between observations of electron cyclotron harmonic (ECH) emissions and observations of chorus. We will work with the CPI and Low Energy Plasma (LEP) teams to find the changes in the particle distribution functions that are associated with the different wave emissions found near the magnetopause.

Recent wave and particle measurements made by instruments onboard the GEOTAIL and POLAR spacecraft have been compared for times when both spacecraft were crossing the same magnetic field lines. GEOTAIL was skimming the magnetopause, and POLAR was at or near one of the northern or southern polar cap boundary layers. The data taken during these times suggest that POLAR instrumentation is observing the effects of high altitude heating of upflowing ionospheric ions, through wave-particle interactions. GEOTAIL observes these same ions after they have propagated into the magnetopause boundary layer through heating and acceleration. These observations, together with solar wind plasma and interplanetary magnetic field measurements from WIND, images of the footprints of the magnetic field from POLAR, and ground-based, remote sensing measurements, will be studied in order to gain a further understanding of the magnetopause boundary layer and the transport and acceleration processes that take place in and near the magnetopause region.

BROADBAND and NARROWBAND ELECTROSTATIC NOISE -- ELECTROSTATIC SOLITARY WAVES

Broadband electrostatic noise (BEN) is a plasma wave phenomenon that dominates the spectrum in the plasma sheet boundary region. Narrowband Electrostatic Noise (NEN) dominates the tail lobe regions. Similar wave emissions to both can be observed in the magnetosheath region. Waveform observations by the GEOTAIL PWI reported in Kojima et al. [1997] were the first to show that the above observed emissions can be divided into the two types of classifications. The BEN type emissions observed in the plasma sheet boundary and magnetosheath consist of series of isolated bipolar pulses. They are termed after their waveforms as "Plasma Sheet Boundary Layer Electrostatic Solitary Waves (PSBL ESW)" and "MagnetoSheath Electrostatic Solitary Waves (MS ESW)." The waveforms of the NEN type emissions are quasi-monochromatic. They are termed as "Lobe Electrostatic Quasi-Monochromatic Waves (Lobe EQMW)" and "MagnetoSheath Electrostatic Quasi-Monochromatic Waves (MS EQMW). The waveform observations with the high time resolution show that one of the common features of these waves is the burstiness. The burstiness means that their amplitudes or frequencies rapidly change in the order of a few milliseconds to a few hundreds of milliseconds. Further, we found from their spin dependence that the PSBL ESW, Lobe EQMW, and MS EQMW are parallel propagating waves relative to the ambient magnetic field. The similarities of the ESW and EQMW in the magnetosheath and magnetotail suggest the possibility that these waves are generated by the same generation mechanism.

Data on electrostatic waves and plasma particles in the deep magnetotail respectively obtained by PWI and CPI onboard GEOTAIL were used to study the generation mechanism of ESW reported in Matsumoto et al. [1997b]. When GEOTAIL experienced multiple crossings of the plasma sheet boundary layer (PSBL) because of the flapping of the magnetotail after a substorm, BEN and Langmuir waves (LW) were observed alternatively. The LW are observed when the velocity distribution function of thermal electrons is relatively cold, while the ESW are observed in association with the hot thermal electrons covering the velocity range of the drift velocity of the assumed electron beam. These plasma

conditions are in agreement with the ESW generation model based on particle simulations. The present study confirms that the ESW are generated by the bump-on-tail instability in the PSBL, and that the ESW travel along the ambient magnetic field being embedded in the high energy tail of the velocity distribution function of the thermal electrons.

Several other studies related to BEN and NEN are in progress. BEN is strongly enhanced near boundary crossings. Frequently Extremely Low Frequency (ELF) electromagnetic waves are observed with enhanced BEN. Yet at other times, the ELF waves and BEN are strongly anti-correlated. The possible association of the low frequency electromagnetic waves and the various electrostatic waves are being studied. We are looking for changes in the particle distributions measured by CPI or LEP that correlate with the observed emissions. The MCA measurements are especially important for these different studies because they extend to a lower frequency than the other PWI receivers and because they provide much better time resolution than the SFA and much more complete temporal coverage than the WFC.

BOW SHOCK and ELECTRON and ION FORESHOCK OBSERVATIONS

GEOTAIL measurements in the Earth's bow shock [Matsumoto et al., 1997a] have identified intense electromagnetic waves in which the magnetic components are at times comparable to the ambient magnetic field. Detailed structures in the ion and electron foreshock regions have also been identified. Electron plasma oscillations (Langmuir waves) and their second harmonic ($2F_p$ emissions) occur in the electron foreshock region upstream of the Earth's bow shock. GEOTAIL has provided both remote sensing and in-situ observations of the terrestrial foreshock to study $2F_p$ emissions [Kasaba et al., 1997a]. The geometry of the $2F_p$ source region was determined by three types of statistical remote sensing analysis: mapping of the $2F_p$ flux, timing analysis of bifurcation phenomena associated with density discontinuities in the solar wind, and propagation direction determined by spin modulation. Three major points were found. The first was that the $2F_p$ source region is on the tangential field line to the bow shock where strong Langmuir waves occur. This provides direct evidence that the 2fp emission is generated from intense Langmuir waves. The second was that both Langmuir waves and $2F_p$ emissions are not strong around the contact point of the tangential field line to the bow shock where acceleration of electrons is expected. This suggests that sharp electron beams are not formed well enough to generate intense Langmuir and $2F_p$ waves because flight time in the region close to the contact point is too short to develop electron beams through the velocity filtering. The third was that the distance of the central position of the source region from the Earth is generally up to 40 R_e. This suggests typical flight length of free energy consumption in the electron beam is sufficient to excite $2F_p$ emissions. These results are consistent with triangular analysis of simultaneous GEOTAIL/PWI and WIND/WAVES observations of $2F_p$ emissions.

We will continue to study the instabilities associated with the Earth's bow shock and foreshock regions. On some days during the deep tail phase of the GEOTAIL mission the

Earth's bow shock was crossed several dozen times. This provides us many opportunities to study the plasma wave characteristics and wave-particle interactions of both the upstream and downstream bow shock phenomena at varying penetration depths. Many crossings of the bow shock also occur now during the near-Earth phase in which GEOTAIL spends extended time just inside or just outside the bow shock. Since all plasma from the sun entering the Earth's magnetosphere must cross the bow shock, better understanding of the wave-particle interactions occurring along the bow shock are critical for meeting the ISTP/GGS goals.

PLASMA WAVE MORPHOLOGY and PLASMA DYNAMICS

GEOTAIL PWI MCA, SFA, and WFC observations have provided high-frequency- and high-time-resolution details of the plasma wave morphology in and the instabilities generated near the regions and boundaries in the magnetosphere and extending out to the deep geomagnetic tail. AKR intensifications when GEOTAIL can view the nightside hemisphere provide excellent indications of substorm onsets. The ideal situation for substorm onset identification would include the simultaneous availability of multiple spacecraft observations of AKR, worldwide ground measurements, and POLAR imaging. Observations of continuum enhancements also provide remote observations of substorms and the resulting plasma dynamics. The combination of the high time-resolution and remote sensing capabilities provided by the plasma wave measurements make them very important for studying the triggering, near triggering, and burstiness of substorms and related geomagnetic disturbances and the resulting plasma dynamics.

An example from May 19, 1993, when GEOTAIL was at XGSE = -161 R_e and YGSE = 27 R_e, clearly demonstrates how the plasma wave data detects the AKR signatures of substorms as well as the resultant plasma dynamics far down the tail. The electric MCA data from 5.6 Hz to 311 kHz (top panel) and magnetic MCA data from 5.6 Hz to 10 kHz (bottom panel) are shown in Figure 4. Enhanced AKR is evident above 100 kHz indicative of substorms, the three strongest beginning around 0700 UT, 1300 UT, and 1830 UT. At the beginning of the day GEOTAIL was in the magnetosheath. The enhanced low frequency electromagnetic signals at or below 20 Hz evident in the magnetic data clearly show when GEOTAIL is in the magnetosheath. The magnetic data show that near each AKR enhancement the low frequency electromagnetic signals disappear indicating that the spacecraft has left the magnetosheath. Data from the SFA will show that at these times GEOTAIL entered a much lower density region. The GEOTAIL particle experiments classify the region as the boundary layer or mantle. Figure 5 displays the SFA data for the same time. The lower cutoff of the trapped continuum radiation is at the local electron plasma frequency, F_p. The relationship is F_p = 9 kHz times the square root of the number density measured in electrons per cc. Before 0700 UT GEOTAIL was primarily in the magnetosheath where F_p exceeded 12.5 kHz. GEOTAIL did briefly encounter the boundary layer a few times before 0700 UT as indicated by the drops in plasma frequency. The strong correlations between the enhanced AKR and the movement of GEOTAIL from the magnetosheath to the boundary layer at around 0700 UT, 1300 UT, and 1830 UT are clear.

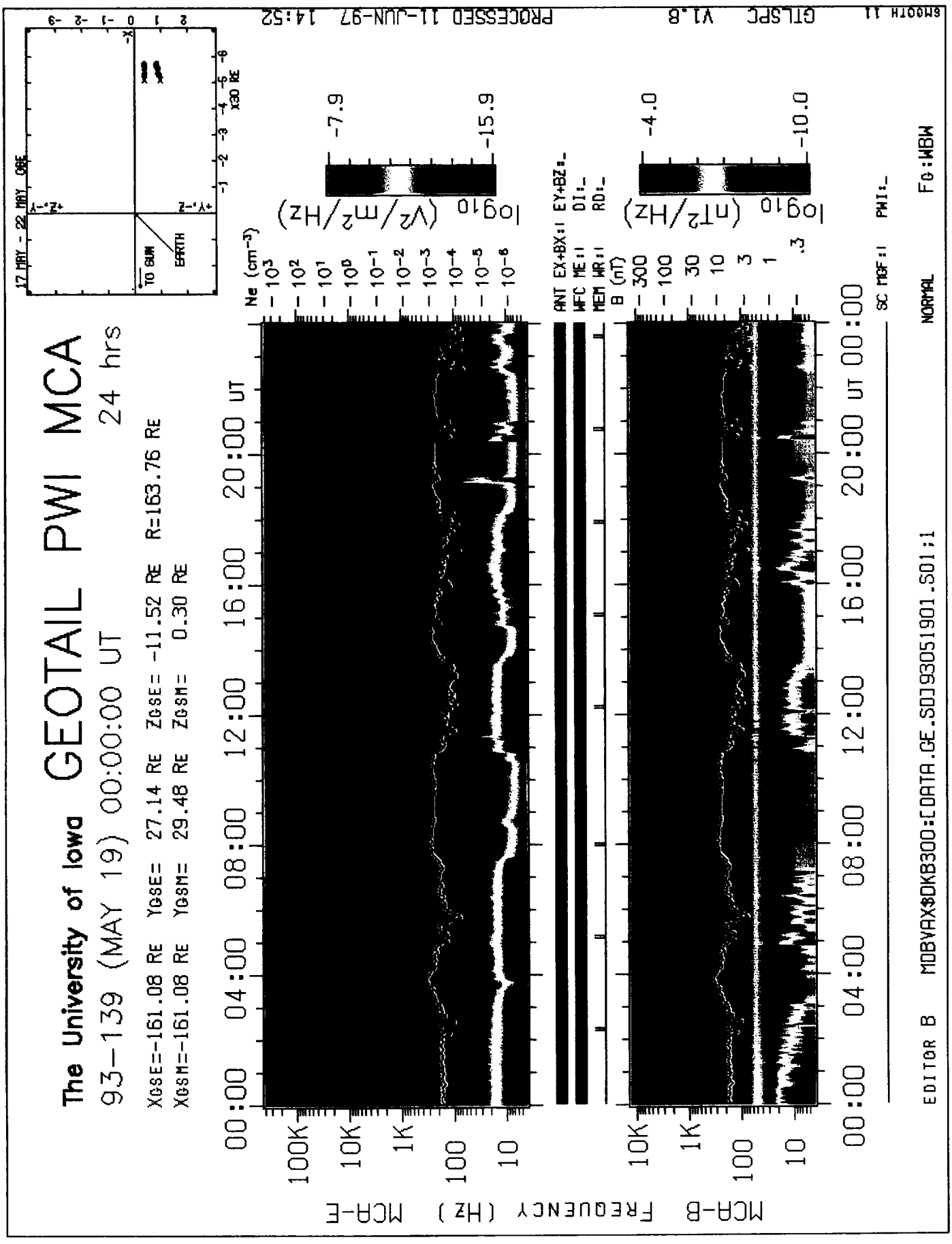
The University of Iowa GEOTAIL PWI MCA
93-139 (MAY 19) 00:00:00 UT
24 hrs
XGSE=-161.08 RE YGSE= 27.14 RE ZGSE= -11.52 RE R=163.76 RE
XGSM=-161.08 RE YGSM= 29.48 RE ZGSM= 0.30 RE
17 MAY - 22 MAY 06E
TO SUN
EARTH
PROCESSED 11-JUN-97 14:52
GTLSPC V1.8
SMOOTH 11
Ne (cm-3)
log10 (V2/m2/Hz)
log10 (nT2/Hz)
ANT EX+BX:! EY+BZ:_
WFC ME:!! DI:_
MEM WR:!! RD:_
B (nT)
MCA-E FREQUENCY (HZ) MCA-B
00:00 04:00 08:00 12:00 16:00 20:00 UT
EDITOR B MOBVAX$DKB300:[DATA.GE.SD193051901.S01;1
NORMAL
SC MOF:!
PHI:_
FG:WBW

Figure 4

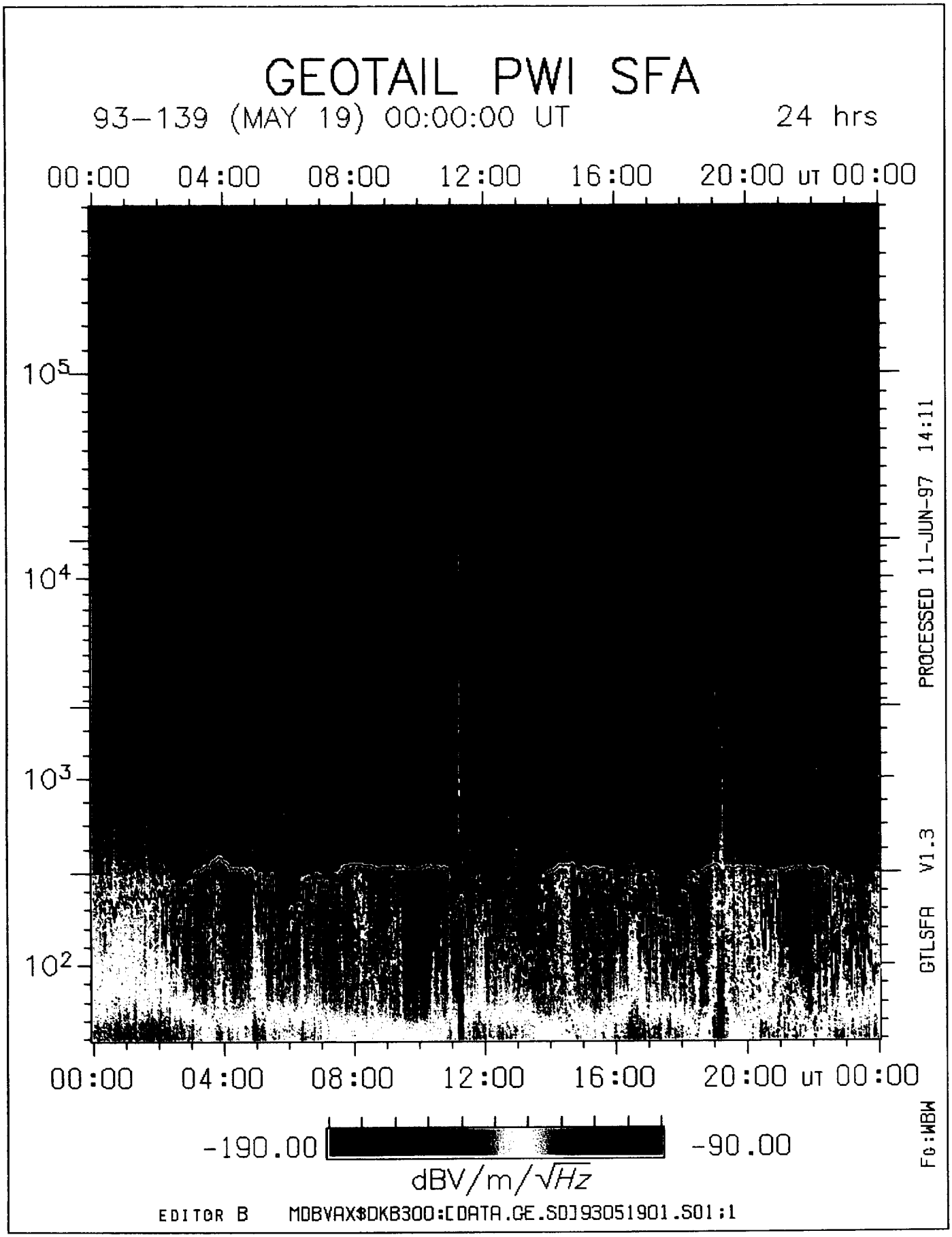
GEOTAIL PWI SFA
93–139 (MAY 19) 00:00:00 UT
24 hrs
00:00 04:00 08:00 12:00 16:00 20:00 UT 00:00
10^5
10^4
10^3
10^2
PROCESSED 11-JUN-97 14:11
GTLSFA V1.3
FG:WBW
-190.00
-90.00
dBV/m/√Hz
EDITOR B MDBVAX$DKB300:[DATA.GE.SDJ93051901.S01;1

Figure 5

The low density and high constant magnetic field (from the GEOTAIL MGF experiment) cause us to describe these actually as crossings into the lobe. At 160 R_e down the tail we are observing the tail expand near the time of the substorm onset. The GEOTAIL PWI observations described here have provided both the remote detection of the substorm onset and the in situ observation of the boundary motions in the tail.

A morphological study with the goal of imaging the magnetosphere and its tail using plasma waves observed with the GEOTAIL PWI MCA experiment is underway. We are conducting a statistical study of the multichannel analyzer electric and magnetic field data for the entire set of GEOTAIL data that we have. The results will help the viewer visualize the intensities of the plasma waves throughout the magnetosphere. The primary goal of this study is to reveal visually the generation and propagation regions of plasma wave emissions throughout the parts of the magnetosphere that GEOTAIL traverses. In addition, this study and similar studies of plasma wave data from spacecraft in complementary orbits will allow techniques to be developed to map plasma densities throughout the magnetosphere using radio sounding. For this study, the magnetosphere was divided into cubical regions (bins) varying in size from 2 R_e on a side to 10 R_e on a side, depending on their location in the magnetosphere. The data values for each frequency (20 electric field from 5.62 Hz to 311 kHz, 14 magnetic field from 5.62 Hz to 10 kHz) for each bin are stored for whenever GEOTAIL is in the bin. This massive statistical data set holds a treasure of information about not only plasma waves, but also about magnetospheric regions and boundaries and the wave-particle interactions that control much of the magnetosphere. The figures plotted from the analysis of these data sets (such as the mean, median, peak, or minimum) will help identify the spatial distributions of the plasma wave emissions throughout most of the magnetosphere. The results of this study can be used to develop techniques to map plasma densities throughout the magnetosphere using radio sounding. In addition, the distribution of the electric and magnetic field spectral densities will be very useful in determining the operational scenarios for radio plasma imaging for the IMAGE space physics mission funded by NASA as a MIDEX project. As an example, continuum radiation may limit, but will certainly not eliminate, the coverage of magnetopause sounding for IMAGE. To determine the extent of this limitation, a joint study of GEOTAIL, POLAR, WIND, and CRRES PWI data could be undertaken.

PLASMOIDS and FLUX ROPES

One subject of great interest to scientists trying to understand substorm dynamics is the plasmoid or flux rope. The PWI and MCA plasma wave measurements help identify and study features associated with plasmoids, flux ropes, and other high speed flow events in the Earth's deep geomagnetic tail. The most common emissions related to them are BEN, NEN, and very low frequency electromagnetic emissions. The frequency of occurrence and intensity of these emissions are strongly dependent on the plasma flow speeds and the plasma temperatures. The BEN and NEN can be quite variable throughout an event. Sometimes NEN which is very intense at very low frequencies but only extends up to a few hundred Hz is prominent. At other times the intensities at the lower frequencies are reduced but the BEN

extends up in frequency to many kHz (typically near the plasma frequency). Occasionally the electrostatic bursts occur as intense discrete rising tones or falling tones. The very low frequency electromagnetic emissions commonly observed are strongest at the lowest detectable frequency of 5 Hz and usually extend up to only a few tens of Hz. Isolated narrow-band electromagnetic emissions in the frequency range from 10's of Hz to around a hundred Hz are sometimes detected. Enhanced Langmuir waves similar to those detected near the earth's bow shock are observed before and after (and occasionally during) the passage of plasmoids in the tail. At the bow shock they are attributed to reflected and accelerated electron beams. This would suggest that the plasmoids have their own boundary and do not remain connected to the earth as they move down the tail. Electrostatic emissions near the electron cyclotron frequency are also occasionally observed. The mixture of broadband and narrowband electrostatic emissions and extremely low frequency electromagnetic waves observed within plasmoids indicates the presence of numerous and varying free energy sources.

We will continue the study of plasma waves observed associated with plasmoids or flux ropes. We are concentrating first on the plasmoids or flux ropes observed on GEOTAIL that have been reported in the literature such as in the Frank et al. [1994] paper. Shinobu Machida and Toshi Mukai from the GEOTAIL LEP investigation have compiled an extensive list of over 800 plasmoid/flux rope events observed on GEOTAIL. They have agreed to share this list with us. We will examine the GEOTAIL MCA and PWI data for these times and correlate it with the MGF, LEP, and CPI data in an attempt to find the source of the many emissions observed.

GEOTAIL PWI MCA RESEARCH PLANS FOR THE UPCOMING YEAR

Many of the various research items discussed above have been reported to the scientific community in papers and presentations at scientific meetings and/or publications in scientific journals and books. These are listed later in this report in the PRESENTATIONS AT SCIENTIFIC MEETINGS and PUBLICATIONS sections. Additional publications on many of the topics are in preparation. In the previous sections we have outlined many of the research topics that we will continue to pursue. Here we will discuss our general research plans for the upcoming year and beyond.

The GEOTAIL PWI experiment along with the POLAR PWI experiment and the WIND WAVES experiment can provide much information on the dynamics of substorms from their remote observations of AKR, Low Frequency (LF) bursts, and continuum radiation emissions received at the three spacecraft in various locations in the magnetosphere and solar wind. A strong correlation between AKR and LF bursts and geomagnetic activity has already been established. Multiple spacecraft observations can now be used to extract inferred plasma dynamics. The frequency limits on the observed AKR and LF bursts are indicative of the altitude of the generation regions. However, these limits could also be affected by high density plasmas between the source and the observing sites. Careful analysis of observations from multiple spacecraft allows us to identify the density and the motion of the intervening

plasmas. Only now do we have sufficient spacecraft to begin separating out the generation and propagation affects. Continuum enhancements related to substorms are believed to be due to the dynamics of the injected particles. Simultaneous observations of continuum enhancements with different time dispersion profiles indicate that the injected particles follow diverse paths. These observations need to be compared with data obtained from the POLAR imagers, the magnetometer and particle data from the geosynchronous satellites, the CANOPUS instruments, and other ground magnetometer data. In some cases the in situ measurements from the magnetometer and particle experiments on GEOTAIL, POLAR, and WIND will also provide useful data regarding the substorm dynamics. Imaging of the Energetic Neutral Atoms (ENA) being carried out using the POLAR CEPPAD detectors could also substantiate the inferences made from the remote plasma wave observations.

A very important reason to extend GEOTAIL and ISTP into the solar maximum period is to identify and compare the significance of various substorm triggering processes. Changes in the IMF and solar wind density and velocity have long been the primary considerations. However, many substorms occur with no obvious change in any of the solar wind parameters. Low frequency (LF) bursts observed by the various ISTP/GGS plasma wave and radio receivers occur simultaneously with intense isolated substorms. Desch and his colleagues on WIND [Desch et al., 1996] found that the LF bursts were well correlated with high solar wind speeds. However, many of the LF bursts we have observed on GEOTAIL occur during moderate solar wind speeds and periods having no obvious change in any of the solar wind parameters. Although a number of scientists remain skeptical, some triggering of AKR by solar type III radio bursts has been substantiated. Wynne Calvert has even suggested that waves (AKR) scattering electrons into the loss cone could be the initiator for some substorms. A more complete understanding of the triggering of substorms should definitely contribute to the space weather initiative.

The majority of the research we have discussed above addresses substorms and/or the effects the sun on the Earth's space weather. Several strong CME events observed since the beginning of 1997 have already produced strong substorms at the Earth that we can study in detail. As we approach solar maximum, these opportunities will increase. Fortunately now both WIND and POLAR have joined GEOTAIL in space. Data from these three and the other GGS/ISTP related spacecraft and ground based investigations will continue to be extremely valuable for studies ranging from high-time resolution wave-particle interactions to more global boundary studies. These data will provide important research opportunities far into the future.

REFERENCES

Anderson, R. R., D. A. Gurnett, H. Matsumoto, K. Hashimoto, H. Kojima, Y. Kasaba, M. L. Kaiser, G. Rostoker, J.-L. Bougeret, J.-L. Steinberg, I. Nagano, and H. J. Singer, Observations of low frequency terrestrial type III bursts by GEOTAIL and WIND and their association with isolated geomagnetic disturbances detected by ground and space-borne instruments, Proceedings of the Planetary Radio Emissions IV Conference, Graz, Austria, in press, 1997a.

Anderson, R. R., D. A. Gurnett, H. Matsumoto, K. Hashimoto, H. Kojima, Y. Kasaba, M. L. Kaiser, G. Rostoker, J.-L. Bougeret, J.-L. Steinberg, I. Nagano, and H. J. Singer, Observations of low frequency terrestrial type III bursts by GEOTAIL and WIND and their association with geomagnetic disturbances detected by ground and space-borne instruments, submitted to Geophys. Res. Lett., 1997b.

Desch, M. D., M. L. Kaiser, and W. M. Farrell, Control of terrestrial low frequency bursts by solar wind speed, Geophys. Res. Lett., 23, 1251-1254, 1996.

Eastman, T. E., S. P. Christon, G. Gloeckler, D. J. Williams, A. T. Y. Lui, R. W. McEntire, E. C. Roelof, T. Doke, L. A. Frank, W. R. Paterson, S. Kokubun, H. Matsumoto, H. Kojima, T. Mukai, Y. Saito, T. Yamamoto, and T. K. Tsurada, Identification of Magnetospheric Plasma Regimes from the Geotail Spacecraft, J. Geophys. Res., to be submitted, 1997.

Frank, L. A., W. R. Paterson, K. L. Ackerson, S. Kokubun, T. Yamamoto, D. H. Fairfield, and R. P. Lepping, Observations of plasmas associated with the magnetic signature of a plasmoid in the distant magnetotail, Geophys. Res. Lett., 21, 2967-2970, 1994.

Kasaba, Y., H. Matsumoto, and R. R. Anderson, GEOTAIL observation of $2F_p$ emission around the terrestrial foreshock region, Adv. in Sp. Res., in press, 1997a.

Kasaba, Y., H. Matsumoto, K. Hashimoto, and R. R. Anderson, The angular distribution of auroral kilometric radiation observed by the GEOTAIL spacecraft, submitted to Geophys. Res. Lett., 1997b.

Kasaba, Y., H. Matsumoto, K. Hashimoto, R. R. Anderson, J.-L. Bougeret, M. L. Kaiser, X. Y. Wu and I. Nagano, Remote sensing of the plasmapause during substorms: GEOTAIL observation of nonthermal continuum enhancement, J. Geophys. Res., submitted for publication, 1997c.

Kojima, H., H. Matsumoto, S. Chikuba, S. Horiyama, M. Ashour-Abdalla, and R. R. Anderson, Geotail waveform observations of broadband/narrowband electrostatic noise in the distant tail, J. Geophys. Res., in press, 1997.

Matsumoto, H., I. Nagano, R. R. Anderson, H. Kojima, K. Hashimoto, M. Tsutsui, T. Okada, I. Kimura, Y. Omura, and M. Okada, Plasma wave observations with GEOTAIL spacecraft, J. Geomag. Geoelectr., 46, 59-95, 1994.

Matsumoto, H., H. Kojima, Y. Kasaba, T. Miyake, R. R. Anderson, and T. Mukai, Plasma waves in the upstream and bow shock regions observed by Geotail, Adv. in Sp. Res., in press, 1997a.

Matsumoto, H., L . A. Frank, Y. Omura, H. Kojima, W. R. Paterson, M. Tsutsui, R. R. Anderson, S. Horiyama, S. Kokubun, and T. Yamamoto, Generation mechanism of ESW based on GEOTAIL plasma wave observation, plasma observation and particle simulation, to be submitted to Geophys. Res. Lett., 1997b.

Yagitani, S., I. Nagano, H. Matsumoto, Y. Omura, W. R. Paterson, L. A. Frank, and R. R. Anderson, Generation and propagation of chorus emissions observed by Geotail in the dayside outer magnetosphere, Proc. of ISAP'96, pp. 717-720, Chiba, Japan, 1996.

PRESENTATIONS AT SCIENTIFIC MEETINGS

The following papers were presented at the XXV General Assembly of URSI held in Lille, France, from 28 August to 5 September, 1996.

Low Frequency Terrestrial "Type III" Bursts Observed Simultaneously by GEOTAIL and WIND, paper H3.3.
R. R. Anderson, H. Matsumoto, K. Hashimoto, Y. Kasaba, M. L. Kaiser, G. Rostoker, J.-L. Bougeret, J.-L. Steinberg, and I. Nagano.

Simultaneous Observation of Wave and Particle by GEOTAIL for Chorus Emissions in the Dayside Outer Magnetosphere, paper H3.P7.
S. Yagitani, I. Nagano, H. Matsumoto, Y. Omura, W. R. Paterson, L. A. Frank, and R. R. Anderson.

The following paper was presented at the Planetary Radio Emissions IV Conference, Graz, Austria, September 1996.

Observations of Low Frequency Terrestrial Type III Bursts by GEOTAIL and WIND and Their Association with Isolated Geomagnetic Disturbances Detected by Ground and Space-borne Instruments.
R. R. Anderson, D. A. Gurnett, H. Matsumoto, K. Hashimoto, H. Kojima, Y. Kasaba, M. L. Kaiser, G. Rostoker, J.-L. Bougeret, J.-L. Steinberg, I. Nagano, and H. J. Singer.

The following papers were presented at the Chapman Conference on "The Earth's Magnetotail: New Perspectives", Kanazawa, Japan, November 1996.

GEOTAIL Observations of Plasma Waves Associated with Plasmoids and Flux Ropes.
R. R. Anderson, H. Matsumoto, H. Kojima, K. Hashimoto, Y. Omura, I. Nagano, S. Kokubun, and T. Yamamoto.

Continuum Enhancement Observed by GEOTAIL: Remote Sensing of the Plasmapause at Substorm.
Y. Kasaba, H. Matsumoto, K. Hashimoto, and R. R. Anderson.

Statistical Analyses of Plasma Waves Observed in the Tail Region: Application of Plasma Waves to the Study of the Geomagnetic Tail Structure.
H. Kojima, H. Hamada, D. Morikawa, H. Matsumoto, T. Murata, R. R. Anderson, T. Yamamoto, and S. Kokubun

Plasma Waves in the Upstream and Bow Shock Regions Observed by GEOTAIL.
H. Matsumoto, H. Kojima, Y. Kasaba, T. Miyake, R. R. Anderson, and T. Mukai

Comparison Between Electron Velocity Distribution Functions and Electrostatic Waves Observed by GEOTAIL.
N. Miki, Y. Omura, T. Mukai, H. Matsumoto, H. Kojima, R. Anderson, Y. Saito, T. Yamamoto, and S. Kokubun.

The following papers were presented at the 1996 Fall Meeting of the American Geophysical Union held in San Francisco, California, in December, 1996.

A Multi-Spacecraft-Multi-Discipline Study of Terrestrial Low Frequency Radio Bursts and Their Relationship to the Dynamics of Geomagnetic Disturbances Detected by Ground and Space-borne Instruments, paper SM12C-11.
R. R. Anderson, D. A. Gurnett, H. Matsumoto, K. Hashimoto, H. Kojima, Y. Kasaba, M. L. Kaiser, G. Rostoker, J.-L. Bougeret, J.-L. Steinberg, I. Nagano, and H. J. Singer.

Remote Sensing and in-situ Observations of the Terrestrial Foreshock: GEOTAIL Observation of 2fp Emission, paper SM71A-7.
Y. Kasaba, H. Matsumoto, M. J. Reiner, R. R. Anderson, and T. Mukai.

Plasma Wave Features on the Bow Shock Ramp, paper SM72F-3.
H. Matsumoto, H. Kojima; D. Morikawa, R. R. Anderson, T. Yamamoto, and T. Okada.

The following papers were presented at the Fifth International School/Symposium for Space Simulation held in Kyoto, Japan, in March, 1997.

Multi-Spacecraft Observations of Terrestrial Low Frequency Radio Bursts and Their Relationship to Other Substorm Monitors.
Roger R. Anderson, Donald A. Gurnett, Hiroshi Matsumoto, Kozo Hashimoto, Hirotsugu Kojima, Yasumasa Kasaba, Michael L. Kaiser, Gordon Rostoker, Jean-Louis Bougeret, Jean-Louis Steinberg, Isamu Nagano, and Howard J. Singer.

Generation and Propagation of Chorus Emissions in the Magnetosphere.
S. Yagitani, I. Nagano, H. Matsumoto, Y. Omura, W. R. Paterson, L. A. Frank, and R. R. Anderson.

Spacecraft Observations and Numerical Simulations of 2fp Waves in the Electron Foreshock.
Y. Kasaba, H. Matsumoto, Y. Omura, R. R. Anderson, T. Mukai, Y. Saito, T. Yamamoto, and S. Kokubun.

Electrostatic Waves Observed in the Geomagnetic Tail: Their Comprehensive Generation Model.
H. Kojima, H. Matsumoto, Y. Omura, H. Furuya, H. Usui, R. R. Anderson, T. Mukai, and Y. Saito.

Comparison Between Electron Velocity Distribution Functions and Electrostatic Waves Observed by GEOTAIL.
N. Miki, Y. Omura, T. Mukai, H. Matsumoto, H. Kojima, R. R. Anderson, Y. Saito, T. Yamamoto, and S. Kokubun.

Generation and Propagation of Chorus Emissions in the Magnetosphere.
S. Yagitani, I. Nagano, H. Matsumoto, Y. Omura, W. R. Paterson, L. A. Frank, and R. R. Anderson.

A Study of Plasma Wave Propagation Based on 3-D MHD Plasmoid Model.
T. Ishikawa. Y. Omura, J. L. Green, H. Matsumoto, M. Ugai, and R. R. Anderson.

Plasma Wave Observations in the Bow Shock and Downstream Regions by GEOTAIL Spacecraft.
D. Morikawa, H. Matsumoto, H. Kojima, T. Yamamoto, T. Mukai, Y. Saito, S. Kokubun, and R. R. Anderson.

The following papers were presented at the Spring Meeting of the American Geophysical Union held in Baltimore, Maryland, in May, 1997.

GEOTAIL, WIND, POLAR, CANOPUS, and ISTP Associated Geosynchronous Satellite Observations of Substorms Following the January 1997 CME Event.
R. R. Anderson, D. A. Gurnett, J. D. Scudder, L. A. Frank, J. B. Sigwarth, H. Matsumoto, K. Hashimoto, H. Kojima, Y. Kasaba, M. L. Kaiser, G. Rostoker, J.-L. Bougeret, J.-L. Steinberg, I. Nagano, H. J. Singer and T. G. Onsager.

Correlative Magnetopause Boundary Layer Observations.
J. S. Pickett, R. R. Anderson, L. A. Frank, D. A. Gurnett, W. R. Paterson, J. D. Scudder, J. B. Sigwarth, B. T. Tsurutani, C. M. Ho, G. S. Lakhina, W. K. Peterson, E. G. Shelley, C. T. Russell, G. K. Parks, M. J. Brittnacher, H. Matsumoto, K. Hashimoto, I. Nagano, S. Kokubun, and T. Yamamoto.

PUBLICATIONS

The journal citation, title, author list and abstract of the publications during this reporting period related to the GEOTAIL PWI MCA investigation are listed below.

The following paper was published in the Proc. of ISAP'96, pp. 717-720, Chiba, Japan, 1996.

Generation and Propagation of Chorus Emissions observed by GEOTAIL in the Dayside Outer Magnetosphere
Satoshi Yagitani, Isamu Nagano, Hiroshi Matsumoto, Yoshiharu Omura, William R. Paterson, Louis A. Frank, and Roger R. Anderson

Abstract. Many chorus emissions have been observed by the GEOTAIL spacecraft, mainly in the dayside outer magnetosphere. The Plasma Wave Instrument (PWI) onboard GEOTAIL makes it possible to examine not only the overall activities of the emissions but also a detailed analysis of wave normal and Poynting directions of each rising/falling frequency tone. During the chorus activities, energetic electrons responsible for the cyclotron generation of the emissions have also been measured by the Comprehensive Plasma Instrument (CPI) with high energy and time resolutions. Comparison between these high-quality in-situ wave/particle data is expected to give experimental evidence to understand complicated nonlinear wave-particle interaction involved in the generation mechanism of the chorus emissions. In this paper, we analyze generation and propagation of chorus emissions observed by the PWI and compare them with simultaneously observed energetic electrons by the CPI, in the dayside outer magnetosphere (near the magnetopause), on October 17-18, 1992. Computing the cyclotron growth rates from the velocity distributions of energetic electrons observed by the CPI, we have shown that the chorus emissions observed by the PWI are most likely generated by those electrons.

The following paper has been accepted for publication in the Journal of Geophysical Research, 1997.

Geotail Waveform Observations of Broadband/Narrowband Electrostatic Noise in the Distant Tail

H. Kojima, H. Matsumoto, S. Chikuba, S. Horiyama, M. Ashour-Abdalla, and R. R. Anderson

Abstract. Broadband Electrostatic Noise (BEN) and Narrowband Electrostatic Noise (NEN) are common wave activities in the plasma sheet boundary and the tail lobe regions, respectively. The similar wave emissions can be observed in the magnetosheath region. We demonstrate the natures of these waves based on the waveform observations by the Plasma Wave Instrument (PWI) onboard GEOTAIL spacecraft. The above observed emissions are divided into the two types of classifications. The BEN type emissions observed in the plasma sheet boundary and magnetosheath consist of series of the isolated bipolar pulses. They are termed after their waveforms as 'Plasma Sheet Boundary Layer Electrostatic Waves (PSBL ESW)' and 'MagnetoSheath Electrostatic Solitary Waves (MS ESW).' On the other hand, the waveforms of the NEN type emissions are quasi-monochromatic. They are termed as 'Lobe Electrostatic Quasi-Monochromatic Waves (Lobe EQMW)' and 'MagnetoSheath Electrostatic Quasi-Monochromatic Waves (MS EQMW).' The waveform observations with the high time resolution show that one of the common features of these waves is the burstiness. The burstiness means that their amplitudes or frequencies rapidly change in the order of a few milliseconds to a few hundreds of milliseconds. Further, we show that the PSBL ESW, Lobe EQMW, and MS EQMW at least are the parallel propagating waves relative to the ambient magnetic field, from their spin dependence. The similarities of the ESW and EQMW in the magnetosheath and magnetotail suggest the possibility that these waves are generated in the same generation mechanism.

The following paper has been accepted for publication in Advances in Space Research, 1997.

Plasma Waves in the Upstream and Bow Shock Regions Observed by Geotail

H. Matsumoto, H. Kojima, Y. Kasaba, T. Miyake, R. R. Anderson, and T. Mukai

Abstract. Upstream waves in the foreshock of the Earth's bow shock are the manifestation of microscopic plasma dynamics caused by the solar wind interaction with the bow shock. Though the past wave observation has revealed many interesting features of the foreshock plasma waves, the lack of important information on the waveforms prevented us from investigating the microphysics of relevant wave-particle interactions beyond certain points. The present paper describes the preliminary results of the GEOTAIL plasma wave observation in the upstream as well as in the bow shock regions. The waveform capture (WFC) receiver has revealed interesting waveforms in these regions which are to provide a clue of understanding the microphysics involved in

the wave generation in the upstream and bow shocks. Based on the observed information, we classify the electron and ion foreshock regions into more detailed structures. We also have carried out some simple computer simulations to understand some of the observed wave phenomena.

The following paper has been accepted for publication in Advances in Space Research, 1997.

GEOTAIL Observation of $2F_p$ Emission Around the Terrestrial Foreshock Region
Y. Kasaba, H. Matsumoto, and R. R. Anderson

Abstract. GEOTAIL is now on the near-tail orbit with an apogee of ~ 30 R_e and a perigee of ~ 10 R_e, and we frequently observe 2fp emissions around the terrestrial electron foreshock by Plasma Wave Instrument (PWI). Since geometric features of the source region should reflect distribution functions of electron beams in the foreshock region, we try to determine geometry of source region of 2fp emission by three kinds of statistical remote sensing analysis: mapping of 2fp flux, timing analysis of bifurcation phenomena associated with solar wind density discontinuities in the solar wind, and propagation direction determined by spin modulation. We confirm three points:

(1) The 2fp source region is on the tangential field line to the bow shock with strong Langmuir waves. This is one piece of direct evidence that 2fp emission is generated from intense Langmuir waves.

(2) Both Langmuir waves and 2fp emissions are not strong around contact point of the tangential field line to the bow shock where acceleration of electrons is expected. This suggests that sharp electron beams are not formed enough to generate intense Langmuir and 2fp waves, because flight time in the region close to the contact point is too short to develop electron beams through the velocity filtering.

(3) Distance of the central position of the source region from the Earth is generally up to 40 R_e. This suggests typical flight length of free energy consumption in the electron beam is enough to excite 2fp emissions.

These results are also consistent with triangular analysis of simultaneous GEOTAIL/PWI and WIND/WAVES observations.

The following paper has been submitted to Geophysical Research Letters, 1997.

The Angular Distribution of Auroral Kilometric Radiation Observed by the Geotail Spacecraft
Y. Kasaba, H. Matsumoto, and K. Hashimoto, R. R. Anderson

Abstract. We use a 38-month data set of GEOTAIL plasma wave observations to analyze AKR at 200 kHz and 500 kHz, and examine the dependence of the angular distribution of auroral kilometric radiation (AKR). We show new results:

(1) The illumination region of AKR extends duskward as geomagnetic conditions become more disturbed especially for the low frequency range.
(2) The frequency of occurrence of AKR depends on observed time in UT which approximately corresponds to the longitude of the source especially for the high frequency range.
(3) AKR is more active on the winter hemisphere especially for the high frequency range.

Possible origins of these dependences are not only the population of energetic electrons on the auroral field lines, but also the structure of the auroral plasma cavity which should be sensitive to plasma density in the surrounding plasmasphere.

The following paper has been submitted to Geophysical Research Letters and is being revised in the editorial process, 1997.

Observations of Low Frequency Terrestrial Type III Bursts by GEOTAIL and WIND and Their Association with Geomagnetic Disturbances Detected by Ground and Space-borne Instruments

R. R. Anderson, D. A. Gurnett, H. Matsumoto, K. Hashimoto, H. Kojima, Y. Kasaba, M. L. Kaiser, G. Rostoker, J.-L. Bougeret, J.-L. Steinberg, I. Nagano, and H. J. Singer

Abstract. In this report we examine a Low Frequency (LF) burst event observed by both the GEOTAIL Plasma Wave Instrument (PWI) and the WIND WAVES experiment while both spacecraft were in the upstream solar wind but at widely separated locations. At the same time the POLAR PWI was at 6 R_e over the northern auroral zone and provided the characteristics of Auroral Kilometric Radiation (AKR) near its source region. These observations are correlated with the CANOPUS ground magnetometer data showing a isolated and moving geomagnetic disturbance near local midnight. In the magnetometer data for GOES 8 which was also near local midnight we have found indications of enhanced field aligned currents and magnetic field dipolarization observed simultaneously with the strong LF burst event. These observations indicate an intimate relationship between AKR, geomagnetic storms, and LF bursts. We suggest that the dynamics of the geomagnetic disturbance may be responsible for some of the observed time dispersion in the LF bursts.

The following paper is being published in Planetary Radio Emissions IV, Proc. Graz Conf., in press, 1997.

Observations of Low Frequency Terrestrial Type III Bursts by GEOTAIL and WIND and Their Association with Isolated Geomagnetic Disturbances Detected by Ground and Space-borne Instruments

Roger R. Anderson and Donald A. Gurnett, Hiroshi Matsumoto, Kozo Hashimoto, Hirotsugu Kojima, and Yasumasa Kasaba, Michael L. Kaiser, Gordon Rostoker, Jean-Louis Bougeret, Jean-Louis Steinberg, Isamu Nagano, and Howard J. Singer

Abstract. The low frequency (LF) terrestrial type III radio burst is a plasma wave emission that typically below 60 to 100 kHz has a smooth time profile and a negative frequency drift. After reviewing past observations, we will examine two LF burst events observed by both the GEOTAIL Plasma Wave Instrument and the WIND WAVES experiment while both spacecraft were in the solar wind and upstream from the Earth's bow shock but at widely separated locations. In both cases enhanced auroral kilometric radiation (AKR) was observed simultaneously with the LF burst by the spacecraft with the least obstructed view of the nightside magnetosphere. The CANOPUS ground magnetometer data and magnetograms from the National Geophysical Data Center (NGDC) show that the LF burst events are well correlated with the expansive phase onsets of intense isolated substorms detected by observing stations near local midnight. In the magnetometer data for GOES 8 we have found enhanced field aligned currents and magnetic field dipolarization observed simultaneously with a strong LF burst event. The recent launch of POLAR has allowed us to detect the AKR very near the source region. Details of the wave observations from WIND, GEOTAIL, and POLAR along with the ground and space magnetometer data indicate an intimate relationship between AKR, geomagnetic substorms, and LF bursts. We suggest that the dynamics of the substorms may be responsible for some of the observed time dispersion in the LF bursts.

The following paper has been submitted to the Journal of Geophysical Research, 1997.

Remote Sensing of the Plasmapause During Substorms: GEOTAIL Observation of Nonthermal Continuum Enhancement

Y. Kasaba, H. Matsumoto, K. Hashimoto, R. R. Anderson, J.-L. Bougeret, M. L. Kaiser, X. Y. Wu and I. Nagano

Abstract. We study continuum enhancement, short-lived enhancement of nonthermal continuum radiation, observed by GEOTAIL spacecraft from November 1994 to December 1995. This radiation is generated at the nightside plasmapause by electrons injected into local midnight zone associated with substorms. We use this radiation as a remote sensing probe for physical processes around the plasmapause during substorms. We find that classical continuum generated at the dayside plasmapause is sometimes observed following the continuum enhancement. This indicates that both are generated by a series of injected electrons associated with the same substorm. Typical interval between the onset of both radiations is $\sim$1 hour, which is consistent with the time lag expected from gradient and curvature drift motion of injected electrons. We also find that some of the continuum enhancement consist of 'fast' and 'main' components, which are distinguished by duration time and rising rate in frequency. We suggest that the fast component is generated first at the plasmapause in local midnight zone by lower energy electrons, while the main component is later generated at the dawnside plasmapause by higher energy electrons. On the other hand, we find that radial distance of the source on the plasmapause, estimated from spacing of banded frequency structure of the continuum enhancement, generally decreases with -0.5 to -1.0 R_e/h for

the first 1 hour after each substorms. Furthermore, we also find that radial distance of the source sometimes increases with +0.1 to +0.5 R_e/h for the next 1 hour associated with isolated substorms in relative quiet phase. The former suggests that long-term decrease of radius of the plasmapause can be separated into fast ones associated with substorms, while the latter suggests that short-term variations of radius of the plasmapause during each substorms is caused not only by the peeling off but also by compression and recovery of the plasmasphere.

The following paper is being submitted to Geophysical Research Letters, 1997.

Generation Mechanism of ESW based on GEOTAIL Plasma Wave Observation, Plasma Observation and Particle Simulation

H. Matsumoto, L . A. Frank, Y. Omura, H. Kojima, W. R. Paterson, M. Tsutsui, R. R. Anderson, S. Horiyama, S. Kokubun, and T. Yamamoto

Abstract. Data on electrostatic waves and plasma particles in the deep magnetotail (X ~ -209R_e) respectively obtained by Plasma Wave Instrument (PWI) and Comprehensive Plasma Instrument (CPI) onboard the GEOTAIL spacecraft were used for the present study. When GEOTAIL experienced multiple crossings of the plasma sheet boundary layer (PSBL) because of the flapping of the magnetotail after a substorm, broadband electrostatic noise (BEN) and Langmuir waves (LW) were observed alternatively. BEN has very fine structures in the dynamic frequency spectra, and their waveforms are in fact a series of electrostatic solitary waves (ESW). The LW are observed when the velocity distribution function of thermal electrons are relatively cold, while the ESW are observed in association with the hot thermal electrons covering the velocity range of the drift velocity of the assumed electron beam. These plasma conditions are in agreement with the ESW generation model based on particle simulations. The present study confirms that the ESW are generated by the bump-on-tail instability in the PSBL, and that the ESW travel along the ambient magnetic field being embedded in the high energy tail of the velocity distribution function of the thermal electrons.

Respectfully Submitted,

Roger R. Anderson